

## Reactivity Inversion in the NiO-O<sub>2</sub> System

G. PARRAVANO

*From the Department of Chemical and Metallurgical Engineering, University of Michigan, Ann Arbor, Michigan 48104*

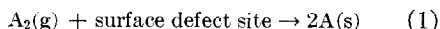
Received April 2, 1968; revised May 16, 1968

The rate of redistribution of carbon-14 between CO and CO<sub>2</sub> has been investigated over NiO catalysts in the temperature range 274° to 450°C, and at  $p_{\text{CO}_2}/p_{\text{CO}}$  ratios 0.1 to 10. Analysis of the results shows that the sign of the relation between the reaction rate and the  $p_{\text{CO}_2}/p_{\text{CO}}$  ratio is a function of temperature and  $p_{\text{CO}_2}/p_{\text{CO}}$  ratio. A thermodynamic model for the description of the gas-solid defect equilibrium has been formulated to explain (a) the reactivity inversion, (b) the numerical values of the mathematical relationship between reaction rate coefficients and the  $p_{\text{CO}_2}/p_{\text{CO}}$  ratio. On the basis of the model, suggestions are advanced for (a) the rate-controlling step of the isotopic exchange reaction, (b) the nature of surface defect sites active in the catalytic reaction and of the adsorbed oxygen intermediate, (c) the slow reaction step and the gas-phase equilibrium controlling the surface concentration of oxygen during the oxidation of CO by O<sub>2</sub> on NiO.

The reactivity reversal is discussed in the framework of the inversion in physicochemical properties that is known to take place in NiO.

The chemical reactivity of a solid surface coexisting with a reactive gas phase is dependent upon thermodynamic as well as kinetic factors. The numerical and energetic aspects of the reactive defect sites at the surface are fixed by thermodynamic conditions while the rate and the stoichiometry of the heterogeneous process are controlled by kinetic factors. Thus, the gas phase exerts a dual influence on the reactivity by determining the number of defect sites and of molecular collisions which will result in a net reaction. The gas-phase pressure governs the extent only of the kinetic influence, while it controls the extent and the *direction* of the thermodynamic effect. It is this latter dual influence which constitutes the central point of this communication.

To define quantitatively the thermodynamic aspect of surface reactivity, let us consider a simple surface defect reaction



where the suffixes g and s refer to gas and surface phases, respectively. In analogy with the formulation of reaction rates in liquid electrolytes, the rate of reaction (1) is expressed by

$$v = k_{\text{rc}} p_{\text{A}_2} \quad (2)$$

and the rate coefficient,  $k_{\text{rc}}$ , is defined by

$$k_{\text{rc}} = k_{\text{a}}[\text{defect site}] \quad (3)$$

where  $k_{\text{a}}$  is the reaction rate constant, dependent upon temperature only. If the surface layer is considered a thermodynamic phase, with A as one of its components, the concentration of defect sites is thermodynamically related to the partial pressure of A<sub>2</sub> namely;

$$[\text{defect sites}] = f(p_{\text{A}_2}) \quad (4)$$

The sign of the function in expression (4) is dependent upon the experimental conditions, gas-phase pressure, and temperature. Therefore,  $k_{\text{rc}}$  [Eq. (3)] may increase or decrease following an increase in  $p_{\text{A}_2}$ . This means that the direction along which the thermodynamic factor influences surface reactivity will depend upon the values of the macroscopic variables. As a consequence of this situation it should be possible to observe under appropriate conditions an inversion in the reactivity pattern of the solid surface. In this study, we wish to present experimental evidence for the presence of a reactivity inversion in the NiO-O<sub>2</sub>

system, to discuss the thermodynamic conditions which control the inversion, and to analyze the implications of these ideas upon surface adsorption and catalytic activity of NiO.

Inversions in solid state transport properties as a function of gas partial pressure are known. For  $1000^{\circ}\text{C} < T < 1200^{\circ}\text{C}$  the  $p$ -type electronic conductivity of  $\text{Cu}_2\text{O}$  was found to decrease with increasing  $p_{\text{O}_2}$ , but for  $T \leq 1000^{\circ}\text{C}$  the conductivity increased with  $p_{\text{O}_2}$  (1). There are also claims that at low  $p_{\text{O}_2}$ , the conductivity becomes independent of  $p_{\text{O}_2}$  (2). Similarly, in FeO at  $T \cong 1300^{\circ}\text{C}$  and high  $p_{\text{O}_2}$  a  $p$ - $n$  transition was detected (3). Electronic inversions, however, cannot directly induce reversal in chemical reactivity, since in the former case electron and electron holes act as charge carriers while electron donors or electron acceptors are involved in surface reactions similar to reaction (1). Thus, a fundamental difference exists between the two effects and the occurrence of one in a given system is not a guarantee for the occurrence of the other in the same system.

A reactivity inversion of thermodynamic origin requires for its detection and study the application of an experimental method which permits following a rate process under conditions of thermodynamic equilibrium between gas and solid surface. This goal can be achieved most conveniently with the use of isotopic exchange reactions. In the case of the reactivity of a metal oxide towards oxygen, the equilibration of oxygen isotopes in molecular  $\text{O}_2$  and of carbon isotopes between CO and  $\text{CO}_2$ , namely,



may be employed. In our study we have made use of results on the rate of reaction (5) over NiO in the temperature range  $274^{\circ}$  to  $450^{\circ}\text{C}$  and at  $p_{\text{CO}_2}/p_{\text{CO}}$  ratios between 0.1 and 10.

#### EXPERIMENTAL

Pure NiO was prepared by slow decomposition of reagent grade  $\text{NiCO}_3$  at temperatures up to  $500^{\circ}\text{C}$  in a stream of dry air for approximately 24 hr, while NiO samples containing Li and Al were made from

standard solutions of the corresponding nitrates, followed by evaporation to dryness and calcination at about  $800^{\circ}\text{C}$ . Although repeated sequences of ball milling and calcination were employed to ensure homogenization of the solid solution, no effort was made to obtain definite proof that solubilization was complete. Surface areas and nominal compositions of the samples employed are summarized in Table 1.

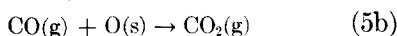
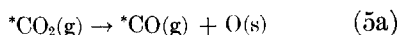
TABLE 1  
BET SURFACE AREAS AND COMPOSITION  
OF NiO SAMPLES

Sample	Addition (mole %)	Surface area ( $\text{m}^2/\text{g}$ )
NiO	—	13.6
NiO + Li	9	3.25
NiO + Al	1	26.9

Before each run, the samples were loaded in the reactor and treated with the  $\text{CO} + \text{CO}_2$  mixture at  $470^{\circ}\text{C}$  for a 10-day period. Because of the chemical equilibrium established during reaction (5) preparative differences among the various samples, a source of great difficulties in previous studies on the reactivity of metal oxides, are considerably minimized or eliminated. The composition of the  $\text{CO} + \text{CO}_2$  mixture was ascertained before and after reaction by mass spectrometric analysis. The rate of reaction (5) was studied in a flow reactor with He as a carrier gas; the reaction conversion was followed by measuring the total radioactivity in  $\text{CO} + \text{CO}_2$  and that in CO. Because of the equilibration pretreatment steady and reproducible results were obtained. No appreciable difference in the rate of reaction (5) was found by inverting the sequence of  $p_{\text{CO}_2}/p_{\text{CO}}$  and/or temperature employed in collecting the results. Details on the equipment and experimental procedure may be found elsewhere (4).

#### RESULTS

The derivation of the rate coefficient for the exchange reaction (5) has been reported previously (5). It is assumed that reaction (5) takes place in a two-step sequence:



Since the transfer of oxygen between CO<sub>2</sub> and CO occurs at equilibrium, the rates of steps (5a) and (5b) are equal. The rate of reaction step (5a) is given by

$$\frac{1}{A} \frac{dn_{*CO}}{dt} = k_{ca} p_{*CO_2} - k'_{ca} p_{*CO} \quad (6)$$

where  $A$ ,  $n_{*CO}$ ,  $k_{ca}$ , and  $k'_{ca}$  are catalyst surface area, moles of  $*CO$ , and rate coefficients of forward and backward reactions of step (a).

The reaction rate expression (6) may be rearranged by introducing the gas flow rate  $v$ , integrating and solving to give the reaction rate coefficient,  $k_{ca}$

$$k_{ca} = \frac{\dot{v}}{ART[1 + (p_{CO_2}/p_{CO})]} \ln \frac{1}{1 - [1 + (p_{CO_2}/p_{CO})][p_{*CO}/(p_{*CO_2})_0]} \quad (7)$$

where the subscript <sub>0</sub> refers to initial conditions.

The influence of the  $(p_{CO_2}/p_{CO})$  ratio on  $k_{ca}$  for pure NiO at 274°, 297°, and 353° and 450°C is reported in Fig. 1, while Figs. 2 and

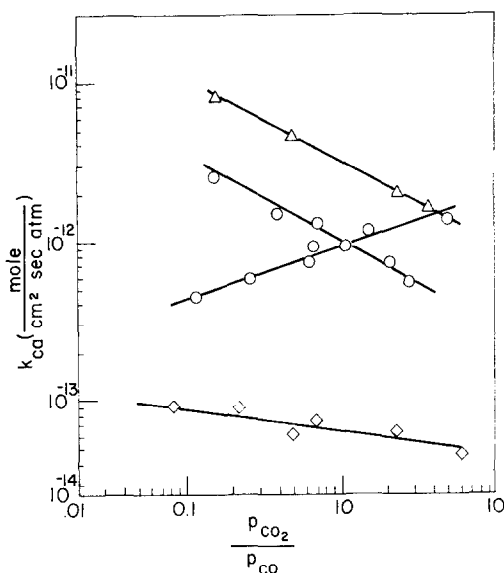


FIG. 1. Influence of  $p_{CO_2}/p_{CO}$  upon the rate coefficient of reaction (5) on pure NiO  $\diamond$ , 274°C;  $\circ$ , 297°C;  $\bullet$ , 353°C;  $\triangle$ , 450°C.

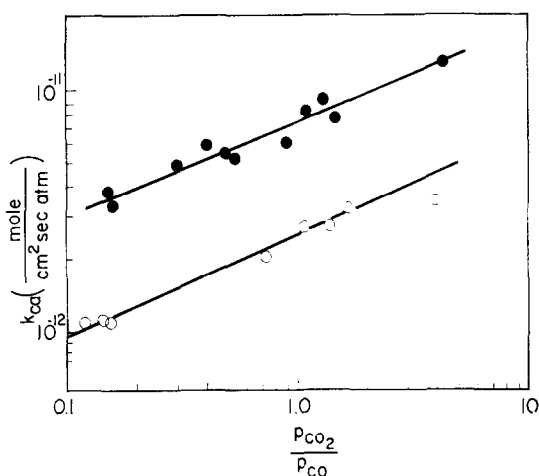


FIG. 2. Influence of  $p_{CO_2}/p_{CO}$  upon the rate coefficient of reaction (5) on NiO + Li  $\bullet$ , 274°C;  $\circ$ , 297°C.

3 present similar information for NiO + Li and NiO + Al. In some experiments, small amounts ( $< 1\%$  by volume) of molecular O<sub>2</sub> were added to the reacting CO + CO<sub>2</sub> mixture. An inhibiting influence on the rate of reaction (5) was noticed for NiO and NiO + Al samples, while no effect was detected for NiO + Li.

In analogy with Eq. (2) the rate expression (6) was written as a first order equation in  $p_{CO_2}$  and  $p_{CO}$  and surface effects which may modify the first order relation are included in  $k_{ca}$  and  $k'_{ca}$ , which are consequently dependent upon  $p_{CO_2}$  and  $p_{CO}$ . The relation between the rate coefficient,  $k_{ca}$ , and the rate constant,  $k_a$ , is expressed as

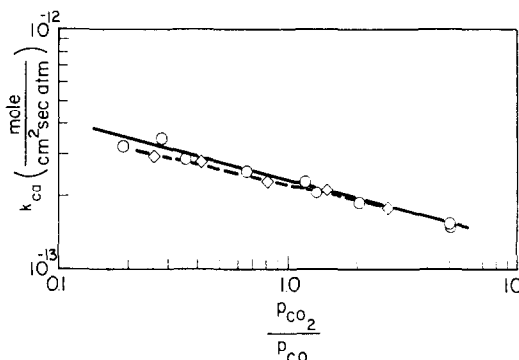


FIG. 3. Influence of  $p_{CO_2}/p_{CO}$  upon the rate coefficient of reaction (5) on NiO + Al,  $\circ$ , 350°C;  $\diamond$ , 374°C.

$$k_{ca} = k_a(p_{CO_2}/p_{CO})^{-m} \quad (8)$$

where  $m$  is a constant. The values of  $m$  computed with the aid of Eq. (8) from experimental results at various temperatures are collected in Table 2.

TABLE 2  
VALUES OF  $m$  [Eq. (8)] FOR REACTION (5)  
CATALYZED BY NiO

Catalyst	Temperature (°C)	$m$
NiO	274°	-0.12
	297°	0.33
	353°	-0.54
	450°	-0.50
NiO + Li	274°	0.42
	297°	0.39
NiO + Al	350°	-0.26
	374°	-0.21

#### DISCUSSION

The significant experimental results reported in the previous section are the following:

(a) In pure NiO,  $k_{ca}$  is influenced by increasing values of the ratio ( $p_{CO_2}/p_{CO}$ ) in three characteristic ways, namely, (i) practically independent at 274°C, (ii) increased at 297°C, and (iii) decreased at 353° and 450°C.

(b) In NiO + Li in the temperature range 274° to 297°C,  $k_{ca}$  increased with increasing ( $p_{CO_2}/p_{CO}$ ) ratios.

(c) In NiO + Al at temperatures 350° and 374°C,  $k_{ca}$  decreased with increasing ( $p_{CO_2}/p_{CO}$ ) ratios.

(d) Significant differences in the numerical values of  $k_a$  are observed for the different samples at the same temperature.

(e) Addition of O<sub>2</sub> to the reaction mixture inhibited the rate of reaction (5) for NiO and NiO + Al, while it did not influence the rate on NiO + Li.

An experimental condition underlying the results of the previous section and of fundamental importance for the present discussion must be emphasized at the outset. In the temperature range 274° to 350°C, the  $p_{CO_2}/p_{CO}$  ratio in equilibrium with NiO coexisting with metallic Ni varies between

10<sup>4</sup> and 10<sup>8</sup>, while the ratio actually employed in our experiments varied approximately between 10<sup>-1</sup> and 10. Thus, the bulk NiO phase was not stable in relation to bulk metallic Ni.

The conditions controlling the dynamic stability and composition of the surface layer of a finely divided phase are not known; it is conceivable, however, to assume that a phase in the NiO-O<sub>2</sub> system intermediate between NiO and metallic Ni, be formed and stabilized under low but finite  $p_{O_2}$  at moderate temperatures. This thermodynamically "reduced" state of NiO can be visualized in various ways. Two of them are of particular interest since they are more amenable to semiquantitative treatment. They are

(a) The formation of interstitial Ni defects in an oxygen excess,  $p$ -type NiO matrix. Clearly, this is unlikely to occur in the NiO bulk phase, because of crystallographic restrictions. Intuitively, however, these restrictions should be greatly relaxed at the surface. These defects are expected to act as donor centers, and to increase the electron population of the solid. The "reduced" character of the solid is thus enhanced.

(b) The formation of singly charged Ni<sup>+</sup> cations at normal lattice position. If this takes place to a sufficient extent in the surface layer, a surface phase corresponding to the stoichiometry of Ni<sub>2</sub>O may be formed.

There is no direct experimental support for the occurrence of either one of these conditions. Reports on the existence of bulk  $n$ -type NiO are contradictory (6, 7), and the onset of ferromagnetism in NiO samples reduced in various ways indicated the presence of minute amounts of metallic Ni (8). On the other hand, recent evidence points to the possibility of preparing oxygen-deficient NiO under suitable reducing conditions. However, it is conceivable that several intermediate states between NiO and metallic Ni with adsorbed O<sub>2</sub> may be stabilized under appropriate experimental conditions, including a surface layer of Ni<sub>2</sub>O in the presence of a CO + CO<sub>2</sub> mixture. If the occurrence of conditions (a) and/or

(b) in the samples investigated is accepted, it is possible to employ them to trace the relation between surface reactivity and  $p_{O_2}$  and to show that the former should vary in a characteristic fashion, bringing about a reactivity reversal of the type discovered in the present study (Figs. 1, 2, 3).

Let us consider first the formation of a surface reduced state through condition (a). The thermal defect reactions\* of interest and the corresponding equilibrium constants are

(i) *atomic disorder*:

$$V_{Ni} + V_0 = 0 \quad (9)$$

$$K_9 = [V_{Ni}][V_0]$$

$$(Ni)_i + V_{Ni} = 0 \quad (10)$$

$$K_{10} = [(Ni)_i][V_{Ni}]$$

$$V_{Ni} = V_{Ni}^{2-} + 2e^+ \quad (11)$$

$$K_{11} = [e^+]^2[V_{Ni}^{2-}]/[V_{Ni}]$$

$$(Ni)_i = (Ni^{2+})_i + 2e^- \quad (12)$$

$$K_{12} = [e^-]^2[(Ni^{2+})_i]/[(Ni)_i]$$

$$V_0 = V_0^+ + e^- \quad (13)$$

$$K_{13} = [V_0^+][e^-]/[V_0]$$

$$V_0^+ = V_0^{2+} + 2e^- \quad (14)$$

$$K_{14} = [V_0^{2+}][e^-]^2/[V_0^+]$$

(ii) *electronic disorder*:

$$e^+ + e^- = 0 \quad (15)$$

$$K_{15} = [e^-][e^+]$$

The extrinsic disorder reactions are

$$\frac{1}{2}O_2(g) = V_{Ni} + O_0 \quad (16)$$

$$K_{16} = [V_{Ni}]/p_{O_2}^{1/2}$$

$$\frac{1}{2}O_2(g) + (Ni)_i = O_0 \quad (17)$$

$$K_{17} = [(Ni)_i]p_{O_2}^{1/2}$$

In addition, the neutrality condition is

$$[e^-] + 2[V_{Ni}^{2-}] = [e^+] + [V_0^+] + 2[V_0^{2+}] + 2[(Ni^{2+})_i] \quad (18)$$

According to the value of  $p_{O_2}$ , five approximations of condition (18) are of interest for the present purpose, namely,

$$[e^+] = 2[V_{Ni}^{2-}](\text{high } p_{O_2})$$

$$[V_0^+] = 2[V_{Ni}^{2-}](\text{medium } p_{O_2})$$

\*These are formulated with the symbolism employed by F. A. Kröger in "Chemistry of Imperfect Crystals," Wiley, New York, 1964.

$$[(Ni^{2+})_i] = [V_{Ni}^{2-}](\text{medium } p_{O_2})$$

$$[V_0^+] = [e^-](\text{low } p_{O_2})$$

$$2[(Ni^{2+})_i] = [e^-](\text{low } p_{O_2})$$

The values of the ratio  $\partial \ln [\text{defect}]/\partial \ln p_{O_2}$ , derived from Eqs. (9) to (17) for the various defects and ranges of condition (18), are summarized in Table 3.

Similar deductions may be derived from condition (b), namely the formation of a reduced phase Ni<sub>2</sub>O. This possibility implies the presence of Ni<sup>+</sup> cations at regular lattice positions and the absence of (Ni<sup>2+</sup>)<sub>i</sub>. In this instance, the important thermal defect reactions are

$$2V_{Ni} + V_0 = 0 \quad (19)$$

$$K_{19} = [V_{Ni}]^2[V_0]$$

$$V_{Ni} = V_{Ni}^- + e^+ \quad (20)$$

$$K_{20} = [V_{Ni}^-][e^+]/[V_{Ni}]$$

together with Eqs. (13), (14), (15), and (16). The neutrality condition is:

$$[e^-] + [V_{Ni}^-] = [e^+] + [V_0^+] + 2[V_0^{2+}] \quad (21)$$

The following limiting cases of condition (21) are noteworthy:

$$[e^+] = [V_{Ni}^-](\text{high } p_{O_2})$$

$$[V_{Ni}^-] = [V_0^+](\text{medium } p_{O_2})$$

$$[e^-] = [V_0^+](\text{low } p_{O_2})$$

From Eqs. (13)–(15), (19), and (20) the values of the ratio  $\partial \ln [\text{defect}]/\partial \ln p_{O_2}$  were calculated for various approximations of condition (21) and are summarized in Table 4.

Inspection of Table 3 shows that upon increasing  $p_{O_2}$  (or the ratio  $p_{CO_2}/p_{CO}$ ) the ratios  $\partial \ln [V_{Ni}^{2-}]/\partial \ln p_{O_2}$  and  $\partial \ln [(Ni^{2+})_i]/$

TABLE 4

VALUES OF  $\partial \ln [\text{defect}]/\partial \ln p_{O_2}$  FROM EQS. (13)–(16), (19), (20) FOR VARIOUS APPROXIMATIONS OF EQ. (21)

Defect	Approximation of Eq. (21)		
	$[e^+] = [V_{Ni}^-]$	$[V_{Ni}^-] = [V_0^+]$	$[e^-] = [V_0^+]$
$[e^-]$	$-\frac{1}{8}$	$-\frac{3}{8}$	$-\frac{1}{4}$
$[e^+]$	$\frac{1}{8}$	$\frac{3}{8}$	$\frac{1}{4}$
$[V_{Ni}^-]$	$\frac{1}{8}$	$-\frac{1}{8}$	0
$[V_0^+]$	$-\frac{3}{8}$	$-\frac{1}{8}$	$-\frac{1}{4}$
$[V_0^{2+}]$	$-\frac{1}{8}$	$\frac{1}{4}$	0

TABLE 3  
VALUES OF  $\partial \ln [\text{defect}]/\partial \ln p_{\text{O}_2}$  FROM EQS. (9)–(17) FOR  
VARIOUS APPROXIMATIONS OF EQ. (18)

Defect	Approximation of Eq. (18)				
	$[e^+] = 2[V_{\text{Ni}^{2-}}]$	$[V_0^+] - 2[V_{\text{Ni}^{2-}}]$	$[(\text{Ni}^{2+})_i] = [V_{\text{Ni}^{2-}}]$	$[V_0^+] = [e^-]$	$2[(\text{Ni}^{2+})_i] = [e^-]$
$e^-$	$-\frac{1}{6}$	$-\frac{1}{6}$	$-\frac{1}{4}$	$-\frac{1}{4}$	$-\frac{1}{6}$
$e^+$	$\frac{1}{6}$	$\frac{1}{3}$	$\frac{1}{4}$	$\frac{1}{4}$	$\frac{1}{6}$
$V_0^+$	$-\frac{1}{3}$	$-\frac{1}{6}$	$-\frac{1}{4}$	$-\frac{1}{4}$	$-\frac{1}{3}$
$V_0^{2+}$	0	$\frac{1}{2}$	$\frac{1}{4}$	$\frac{1}{4}$	0
$V_{\text{Ni}}^{2-}$	$\frac{1}{6}$	$-\frac{1}{6}$	0	0	$\frac{1}{6}$
$(\text{Ni}^{2+})_i$	$-\frac{1}{6}$	$\frac{1}{6}$	0	0	$-\frac{1}{6}$

$\partial \ln p_{\text{O}_2}$  change sign. In particular, for the approximation  $2[V_{\text{Ni}}^{2-}] = [V_0^+]$ ,  $[V_{\text{Ni}}^{2-}]$  decreases and  $[(\text{Ni}^{2+})_i]$  increases with increasing  $p_{\text{O}_2}$ . This is contrary to what one would expect and it is the result of the presence of the double charge of one of the vacancies. This condition is similar to that observed in BaO. Similarly, Table 4 shows that the dependence of  $[V_{\text{Ni}}^-]$  and  $[V_0^{2+}]$  upon  $p_{\text{O}_2}$  changes direction as  $p_{\text{O}_2}$  is increased. In this case the unexpected result that  $[V_{\text{Ni}}^-]$  decreases and  $[V_0^{2+}]$  increases with increasing  $p_{\text{O}_2}$  is a consequence of the form of the Schottky product in Eq. (19). This situation is analogous to that present in  $\text{Cu}_2\text{O}$  (1).

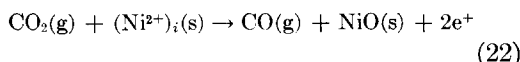
The question may be asked whether generalizations for the occurrence of these unusual effects are possible. With the limited amount of information available, it seems that in pure ionic compounds the effects arise from asymmetry in the position of the energy levels of the controlling defects with respect to the valence and conduction bands. Consider a metal oxide,  $\text{MeO}$ , containing  $V_{\text{Me}}^-$ ,  $(\text{Me}^{2+})_i$ , and  $(\text{Me}^+)_l$  ionic defects.  $V_{\text{Me}}^-$  is located above the valence band at a distance similar to that between  $(\text{Me}^{2+})_i$  levels and the conduction band. In addition,  $(\text{Me}^+)_l$  levels are present and located closer than  $(\text{Me}^{2+})_i$  levels to the conduction band. At low temperature (or low  $p_{\text{O}_2}$ ), the former will be the predominant defects and, expressing the extrinsic defect equilibrium as  $\frac{1}{2} \text{O}_2(\text{g}) + (\text{Me}^+) = \text{MeO}(\text{s})$ , the well-known result  $[(\text{Me}^+)_{l,i}] \propto (p_{\text{O}_2})^{-1/2}$  is obtained. At high temperature, (or high  $p_{\text{O}_2}$ ) however,  $V_{\text{Me}}^-$  and  $(\text{Me}^{2+})_i$  are the stable species and the condition  $[V_{\text{Me}}^-] \cong 2[(\text{Me}^{2+})_i]$  is valid. The extrinsic defect equilibrium is then

written as  $\frac{1}{2} \text{O}_2(\text{g}) + \text{Me}(\text{s}) = \text{O}_0 + 2V_{\text{Me}}^- + (\text{Me}^{2+})_i$ , giving  $[(\text{Me}^{2+})_i] \propto p_{\text{O}_2}^{1/6}$ . In this range an increasing  $p_{\text{O}_2}$  will increase the concentration of  $(\text{Me}^{2+})_i$ , contrary to what one may expect and opposite to the behavior of the low-temperature range. At present the knowledge of the defect equilibrium constants for bulk reactions is limited. There is no possibility to indicate values for surface equilibrium constants even in an approximate fashion. The possibility of complicating factors arising from local electrical conditions cannot be overlooked. As a result, the ranges of  $p_{\text{O}_2}$  which correspond to the various approximations of the neutrality equations (18) and (21) cannot as yet be predicted. Similarly, the choice between the two models characterized by conditions (a) or (b) to fit the experimental results can only be done on the basis of factual considerations. In this instance, as discussed below, the comparison between the expected and the experimental numerical values of  $m$  is a guide.

The previous conclusions may be applied to the experimental results of the previous section. In the temperature range studied the virtual  $p_{\text{O}_2}$ , in equilibrium with the NiO samples, varied by about 10 orders of magnitude. It is suggested that as the virtual  $p_{\text{O}_2}$  changed with the reaction temperature, the various ranges of validity of the neutrality equations (18) and (22) were established within the surface layer of the NiO samples.

Let us consider condition (a) [formation of  $(\text{Ni}^{2+})_i$  defects in pure NiO] and let us assume that the condition of the NiO surface layer was such that the approximations of the electrical neutrality equa-

tions (18) were established as the temperature increased from 274° to 450°C. If we assume, further, that  $(\text{Ni}^{2+})_i$  were the surface defects responsible for the catalytic activity in reaction (5), the inversion of the former is readily explained. In fact, writing the rate-controlling step of reaction (5) as



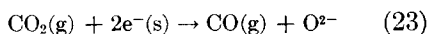
from Table 3, approximation  $[(\text{Ni}^{2+})_i] = [V_{\text{Ni}}^{2-}]$ , the rate coefficient of reaction (5) is

$$k_{\text{ca}} = k_a[(\text{Ni}^{2+})_i] = k_a(p_{\text{CO}_2}/p_{\text{CO}})^0 = k_a$$

at lower temperature. As the temperature increased conditions for the validity of the approximation  $[V_{\text{O}}^+] = [V_{\text{Ni}}^{2-}]$  (Table 3) were set up, or

$$k_{\text{ca}} = k_a(p_{\text{CO}_2}/p_{\text{CO}})^{1/3}$$

At still higher temperatures (approximation  $[e^+] = [V_{\text{Ni}}^{2-}]$ ) a rate-controlling step



gives  $k_{\text{ca}} = k_a (p_{\text{CO}_2}/p_{\text{CO}})^{-2/3}$ . These conclusions are in satisfactory agreement with the results reported in Table 2 for pure NiO. On the basis of this interpretation the addition of Li to NiO extended the range of validity of the approximation  $[V_{\text{O}}^+] = [V_{\text{Ni}}^{2-}]$  toward higher  $p_{\text{O}_2}$ . This may be the consequence of higher  $\text{Ni}^{2+}$  levels and lower energy of defect formation. Assuming for NiO + Li samples a rate-controlling step similar to that postulated for pure NiO samples [reaction (22)], the rate coefficient on the former catalysts becomes  $k_{\text{ca}} = k_a (p_{\text{CO}_2}/p_{\text{CO}})^{1/3}$  in fair numerical but correct sign agreement with the experimental results (Table 2).

Al addition had the effect of decreasing the numerical values of  $m$  (Table 2) to about one-half of the values corresponding to pure NiO. The lower values of  $m$  can only be accounted for by means of the results from model (b) (Table 4). Al dissolution into NiO may be considered as a reduction since  $[e^+]$  is decreased. In this case, it is suggested that direct reduction of  $\text{Ni}^{2+}$  to  $\text{Ni}^+$  ions takes place, and that the model underlying condition (b) is more appropriate to describe the ionic and electronic

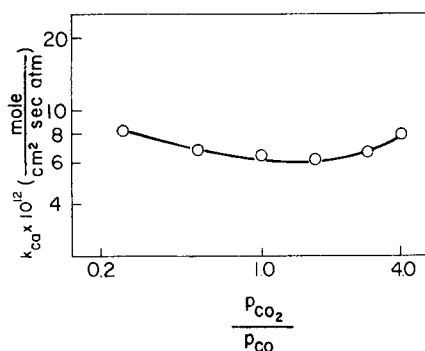
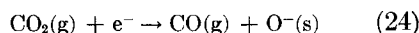


FIG. 4. Influence of  $p_{\text{CO}_2}/p_{\text{CO}}$  upon the rate coefficient of reaction (5) on pure NiO at 525°C.

conditions of the surface layer. It is not possible to offer a fundamental explanation for the change of models required by the addition of 1 mole % Al. Many suggestions and speculations may be advanced with little or no possibility of justifying them experimentally. Using the approximation  $[e^+] = [V_{\text{Ni}}^{2-}]$  for the neutrality equation (21) and assuming a rate-controlling step as



one obtains an expression for the reaction rate coefficient,  $k_{\text{ca}} = k_a (p_{\text{CO}_2}/p_{\text{CO}})^{-1/4}$  in good agreement with the experimental results (Table 2).

In the previous discussion, the possible influence of isothermal changes of the ratio  $p_{\text{CO}_2}/p_{\text{CO}}$  upon the defect structure of the surface has been neglected, since the range of ratios covered in the experiments was about one order of magnitude only. It is, however, conceivable that a reactivity inversion under isothermal conditions may take place as a consequence of variations in the  $p_{\text{CO}_2}/p_{\text{CO}}$  ratio only. In this instance, plots of  $\log k_{\text{ca}}$  versus  $\log (p_{\text{CO}_2}/p_{\text{CO}})$  will have a maximum or a minimum. This behavior was indeed observed at higher temperatures (Fig. 4). This shows that the actual defect situation in the surface layer may become more complex than that represented by the models (a) and (b) and that additional defect interactions should be considered. These refinements, however, will not add substantially to the basic interpretation of the reactivity reversal, as set forth in this paper.

It is instructive to compare the values of the rate constants,  $k_a$ , among the various samples. These values have been calculated by means of Eq. (8) and are reported in Table 5.

TABLE 5  
VALUES OF THE RATE CONSTANT,  $k_a$ , FOR  
REACTION (5) CATALYZED BY NiO

Catalyst	Temperature (°C)	$\left(\frac{k_a}{\text{cm}^2 \text{ sec atm}}\right)$
NiO	274°	$6.5 \times 10^{-14}$
NiO + Li	274°	$3.0 \times 10^{-12}$
NiO	297°	$9.0 \times 10^{-13}$
NiO + Li	297°	$7.4 \times 10^{-11}$
NiO	350°	$1.0 \times 10^{-12}$
NiO + Al	350°	$2.8 \times 10^{-13}$

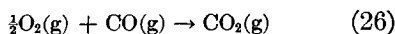
Table 5 shows that the addition of Li had the effect of increasing the value of  $k_a$  by about two orders of magnitude at 274°C and one order of magnitude at 297°C, while the addition of Al decreased the value of  $k_a$  by one order of magnitude at 350°C. The results suggest also differences in the reaction activation energies.

Because of the method followed in the derivation of the values of  $k_a$  (Table 5), a direct influence on the latter of the electronic and ionic disorder of the solid is eliminated. In contrast to the majority of past studies on the effect of solid additions to the catalytic activity of NiO, the interpretation of the addition effect found in this study must be sought in more subtle phenomena than in the nature and extent of the change in the electronic and ionic disorders of NiO brought about by the addition. To carry out this analysis results covering a larger range of conditions are needed.

In the experiments covering the addition of molecular O<sub>2</sub> to the reacting CO + CO<sub>2</sub> mixture, the reaction step



must be considered together with reaction steps (5a) and (5b). The combination of reaction steps (5a) [or (5b)] and (25) results in the catalytic oxidation of CO.



If under reaction conditions, the O<sub>2</sub> equilibrium [reaction step (25)] is rapidly established in relation to the CO-CO<sub>2</sub> equilibrium [reaction step (5b)], the rate of formation of \*CO [reaction step (5a)] will be reduced by O<sub>2</sub> additions to the feed gases. In this instance \*CO will be more rapidly oxidized by O<sub>2</sub> than produced from \*CO<sub>2</sub> and the steady state concentration of oxygen at the surface during CO oxidation will be controlled by the O<sub>2</sub> equilibrium [step (25)] or  $[\text{O}(\text{s})_{\text{ss}}] \cong [\text{O}(\text{s})_{\text{c}}]$ . Conversely, if O<sub>2</sub> additions will not influence the rate of reaction (5), the surface concentration of oxygen at steady state will be controlled by the CO-CO<sub>2</sub> equilibrium, or  $[\text{O}(\text{s})_{\text{ss}}] \cong [\text{O}(\text{s})_{(\text{a})}]$ . The experimental results reported in the previous section for pure NiO and NiO + Al support the establishment of the first of these two possibilities. This conclusion is in excellent agreement with direct studies on the rate of oxidation of CO on NiO performed several years ago (9). These investigations showed that at temperatures > 200°C the rate-controlling step was indeed the removal of adsorbed oxygen by reaction with CO. No influence on the rate of reaction (5) by O<sub>2</sub> addition was detected on NiO + Li samples. This would indicate that, in this case, the CO-CO<sub>2</sub> equilibrium governs the chemical potential of adsorbed oxygen. However, a more direct evidence for this conclusion must be obtained from experiments on the rate of reaction (5) using as a feed gas \*CO instead of \*CO<sub>2</sub>, as performed in this work.

## CONCLUSION

The presence of an inversion in the surface reactivity of NiO has been demonstrated experimentally and traced to the operation of thermodynamic factors in the defect chemistry of the solid. Thus, under appropriate conditions, the concentration of bare surface sites for the adsorption of O<sub>2</sub> increases with increasing  $p_{\text{O}_2}$ .

At first sight, this is a rather unexpected phenomenon. However, if the result is viewed under the dual role of poison and promoter, that adsorbed oxygen is known to play in catalytic oxidations, the effect is cast into a more familiar pattern. (Ni<sup>2+</sup>),



ions, which at the surface may be considered as adsorbed Ni<sup>2+</sup> ions, are the active surface sites at lower temperatures for the transfer of oxygen between CO and CO<sub>2</sub> [Eq. (22)], while electrons become kinetically significant at higher temperatures [Eqs. (23) and (24)]. In both instances, the preponderant form of adsorbed oxygen is O<sup>2-</sup>. Li addition to NiO, acting as oxidizing agent, extends to higher temperatures the reactivity behavior of pure NiO, while Al addition promotes a reduction of Ni<sup>2+</sup> ions at regular lattice sites. As a result of these effects the dependence of the chemical reactivity of NiO upon  $p_{O_2}$  and the rate constant for the oxygen transfer between CO and CO<sub>2</sub> may be controlled by the dissolution into the bulk phase of alter ions.

These results should be viewed in the more general framework of the known inversion of physicochemical properties of NiO.

Several years ago, it was shown that inversions in the lattice constant, density, electronic conductivity, and related physicochemical properties take place as a function of Li addition to NiO (10). The inversion of physicochemical properties was indeed discussed in connection with an inversion in catalytic behavior. At that time, the only catalytic property of the NiO-O<sub>2</sub> system available for a theoretical analysis was the activation energy for the oxidation of CO, a parameter of complex and marginal significance for direct interpretation. Yet, that early suggestion has been remarkably confirmed and clearly supported by the more sophisticated approach employed in this work.

Despite the crudeness of the models employed in this study and the neglect of chemical and electrical interaction effects in the formulation of surface defect equilibria, the inversion effect discussed in this paper should be of general occurrence whenever the thermodynamic conditions during reaction induce a defective surface layer whose general characteristic is the asymmetric

position of the electronic levels of the controlling solid state defects.

#### ACKNOWLEDGMENTS

I wish to express my thanks to Mr. D. Y. Cha for obtaining the experimental results on reaction (5) reported in this paper and to the National Science Foundation for financial support of this study.

#### REFERENCES

1. BLOEM, J., *Philips Res. Repts.* **13**, 167 (1958).
2. GUNDERMANN, J., HAUFFE, K., AND WAGNER, C., *Z. Phys. Chem.* **B37**, 148 (1937); BOTTGER, O., *Ann Phys.* **10**, 232 (1952); TOTH, R. S., KILKSON, R., AND TRIVICH, D., *Phys. Rev.* **122**, 482 (1961); O'KEEFE, M., AND MOORE, W. J., *J. Chem. Phys.* **35**, 1324 (1961).
3. TANNHAUSER, D., *J. Phys. Chem. Solids* **23**, 25 (1962); GEIGER, G. H., LEVIN, R. L., AND WAGNER, J. B., JR., *J. Phys. Chem. Solids* **27**, 947 (1966); SWAROOP, B., AND WAGNER, J. B., JR., *Trans. Met. Soc. AIME* **239**, 1215 (1967); HILLEGAS, W. J., AND WAGNER, J. B., JR., *Phys. Letters* **25A**, 742 (1967).
4. CHA, D. Y., AND PARRAVANO, G., to be published.
5. GRABKE, H. J., *Proc. Intern. Congr. Catalysis, 3rd, Amsterdam, 1964*, p. 928; *Z. Elektrochem.* **69**, 48 (1965).
6. SCHLOSSER, E. G., *Z. Elektrochem.* **65**, 453 (1961); HAUFFE, K., in "Transition Metal Compounds," Proceedings of the Buhl International Conference on Materials, Pittsburgh, Pennsylvania, 1963, p. 37. Carnegie Institute of Technology.
7. VAN HOUTEN, S., in "Transition Metal Compounds," Proceedings of the Buhl International Conference on Materials, Pittsburgh, Pennsylvania (1963), Carnegie Institute of Technology, p. 49.
8. KLEMM, W., "Magnetochemie." Akademische Verlagsgesellschaft M. B. H., Leipzig, 1933.
9. PARRAVANO, G., *J. Am. Chem. Soc.* **75**, 1352, 1448 (1953).
10. PARRAVANO, G., AND BOUDART, M., *Advan. Catalysis* **7**, 47 (1955).
11. SCHLOSSER, E. G., AND HERZOG, W., paper presented at the Fourth International Congress on Catalysis, Moscow, 1968, Paper no. 9.